On mean field theory for ac-driven elastic interfaces exposed to disorder

Friedmar Schütze*

Institut für Theoretische Physik, Universität zu Köln, Zülpicher Straße 77, 50937 Köln, Germany

(Dated: November 20, 2018)

The analytic description of ac-driven elastic interfaces in random potentials is desirable because the problem is experimentally relevant. This work emphasises on the mean field approximation for the problem at zero temperature. We prove that perturbation theory is regular in all orders by giving an inductive scheme how to find groups of ill-behaved graphs that mutually cancel, leaving a regular expression. In the parameter regimes for which perturbation theory is applicable it agrees with numerical results. Further, we determine the dependence of the Fourier coefficients of the mean velocity on the parameters of the model.

PACS numbers: 46.65.+g, 75.60.Ch, 02.30.Mv

I. INTRODUCTION

The theory for elastic interfaces in a disordered environment, driven by an external dc-force at temperature $T = 0$ is widely understood, and also in the finite temperature case some progress has been achieved [1, 2, 3, 4, 5, 6]. At $T = 0$ the dc driven interface exhibits an interesting critical point, corresponding to the depinning transition. For small constant driving forces h, the interface adjusts its configuration to balance the driving force and the disorder, but remains pinned and does not move on large time scales. If h reaches a critical threshold h_{p}, the interface starts to slide with a mean velocity v that behaves as $v \sim (h - h_{\mathrm{p}})^{\beta}$ for $h \searrow h_{\mathrm{p}}$. The critical properties of this non-equilibrium transition have been worked out by the use of functional renormalisation group methods [7, 8, 9, 10, 11, 12, 13].

Beyond constant driving forces, experimental achievements on the problem of ac-driven elastic domain walls in ferroic systems [14, 15, 16] emphasise the importance of a theoretical understanding. Despite the experimental progress, and in contrast to the success in understanding the dc case, yet there is little advance in the theoretical description of the problem, even for $T = 0$. The exact solution of the equation of motion is deemed impossible due to the complicated non-linear feedback of the interface's configuration in the disorder force term. To make matters worse, attempts to access the problem for an ac-driving force perturbatively by an expansion in the disorder strength bring along severe problems [17].

This underlines the importance of the mean-field approach, which is the central subject of this article. We investigate the behaviour of ac-driven domain walls in a disordered environment in the mean-field approximation and prove, that the perturbative corrections remain bounded in all orders. Further, we indicate, that for large enough driving field amplitudes, sufficiently strong elastic coupling and high frequencies, the perturbative results agree very well with the numerics for the full mean field

equation of motion. The quantitative statements that rely on a special choice for the disorder correlator are worked out for elastic manifolds, like for example interfaces between two immiscible fluids or domain walls in ferroic systems, exposed to random field disorder. Our proof of the regularity of perturbation theory should also extend to similar models that describe other interesting physical systems with disorder [18, 19], for example charge-density waves [20] and flux lines in type-II superconductors [21, 22, 23].

Mean field calculations have been performed for similar problems before. D.S. Fisher [24, 25] calculated dynamic properties of sliding charge-density waves in a mean-field model with dc-driving and argued in favour of a depinning transition in the strong pinning case. Using smooth bounded disorder, he calculated the threshold field for depinning as well as critical exponents related to the depinning transition. Furthermore, he considered the response in case of an ac-field applied in addition to the dc-driving. The perturbation expansion for dc-driven interfaces has been investigated by Koplik and Levine [26], who also emphasised on the mean-field problem. Later, Leschorn [27] calculated the depinning force and the critical properties of the depinning transition for a three-state random field model. Narayan and Fisher [8] investigated the critical behaviour of charge density waves in the sliding regime and worked out the threshold field for scalloped disorder potentials. Lyuksyutov considered dynamical friction and instability phenomena for the interface motion [28].

The rest of this article is organised in the following way: In the next section, we are going to deduce the mean-field equation of motion from the original model taken to describe the problem of disordered elastic domain walls. In section III, we establish the diagrammatic perturbation expansion for the mean-field theory and show its regularity. The bulk part of the inductive proof (the induction step) is outsourced to the appendix. After a brief review of the problem for a constant driving force in section IV, we focus our attention to the ac-driving case in section V. There, we start with some qualitative discussion of the numerical solution and then go on to present our attempts to extract information from the first non-

*Electronic address: schuetze@thp.uni-koeln.de

vanishing perturbative terms. Due to the complicated non-linear structure of the expressions involved, numerical methods had to be employed as well. However, the perturbative approach helps a lot to improve numerical results. This makes it possible to work out the decay law of the Fourier coefficients with their order, in dependence of the strength of the driving field.

II. THE MODEL

To model D-dimensional elastic manifolds in a $D+1$-dimensional disordered system, we employ an equation of motion that has been introduced in a number of earlier works [26, 29, 30]

$$\partial_t z(x,t) = \Gamma \nabla_x^2 z + h \cdot f(t) + u \cdot g(x,z). \quad (1)$$

The equation does not involve a thermal noise term and therefore describes the (classical) system at $T=0$. The interface profile is described by the single-valued function $z(x,t)$, so we do not allow for overhangs. Here, x is the D-dimensional set of coordinates which parameterise the interface manifold itself. Γ denotes the elastic stiffness constant of the interface, h measures the strength of the external driving force and $f(t)$ denotes its time-dependence, taken to be of order unity. We did not specify $f(t)$ yet to allow for general considerations. The disorder is modeled by $g(x,z)$, its strength is measured by u. We assume quenched Gaußian disorder, characterised by its first two cumulants:

$$\langle g(x,z) \rangle = 0,$$
$$\langle g(x,z)g(x',z') \rangle = \delta^D(x-x')\Delta(z-z'). \quad (2)$$

Here, $\langle \ldots \rangle$ denotes the average over disorder. The function $\Delta(z)$ will be specified further down. As the short-ranged elastic term suggests, long-range interactions, of dipolar type for example, are not covered.

The corresponding mean field equation (cf. e.g. [25]) is obtained via the replacement of the elastic term by a uniform long-range coupling. To do this, we have to formulate the model (1) on a lattice in x-direction, i.e. the coordinates that parameterise the interface itself are discretised. The lattice Laplacian reads

$$\nabla_x^2 z(x_i) = \sum_{d=1}^{D} \frac{z(x_i+ae_d)+z(x_i-ae_d)-2z(x_i)}{a^2}$$
$$= \sum_{d=1}^{D}\sum_{j_d=1}^{N} J_{ij_d}\left[z(x_{j_d})-z(x_i)\right],$$
$$J_{ij_d} = \frac{1}{a^2}\left[\delta_{j_d+1,i}+\delta_{j_d-1,i}\right],$$

where a denotes the lattice constant. To get the mean field theory, J_{ij} has to be replaced by a uniform coupling but such that the sum over all couplings $\sum_j J_{ij}$ remains

the same. Hence, we choose

$$J_{ij}^{\mathrm{MF}} = \frac{1}{a^2 N}. \quad (3)$$

Now, the disorder has to be discretised as well, which is achieved if we replace the delta function in the correlator (2) by $\delta^D(x_i-x_j) \to \delta_{ij}a^{-D/2}$ (cf. [30]). The resulting equation of motion should be independent of x, just the lattice constant a and the dimension enter because the disorder scales with a factor $a^{-D/2}$. Finally, for the mean-field equation of motion, we obtain

$$\partial_t z = c \cdot [\langle z \rangle - z] + h \cdot f(t) + \eta \cdot g(z), \quad (4)$$

where $c = \Gamma/a^2$ and $\eta = u/a^{D/2}$. We assume quenched Gaußian disorder with

$$\langle g(z) \rangle = 0 \quad (5)$$
$$\langle g(z)g(z') \rangle = \Delta(z-z'). \quad (6)$$

The function $\Delta(z-z')$ shall be smooth, symmetric and should decay exponentially on a length scale ℓ. Moreover, we require $\Delta(0)=1$, as the disorder strength shall be measured by η. For the sake of concreteness, we shall choose

$$\Delta(z-z') = \exp\left[-\left(\frac{z-z'}{\ell}\right)^2\right] \quad (7)$$

whenever we need an explicit expression for calculations. This disorder correlator correctly describes the situation for an elastic manifold in random field disorder [10], sufficiently far away from the critical depinning transition point.

The physical picture of the mean field equation of motion is a system of distinct particles, moving in certain realisations of the disorder. All of them are harmonically coupled to their common mean, i.e. the elastic coupling between neighbouring wall segments $\Gamma\nabla_x^2 z$ is now replaced by a uniform coupling $c \cdot [\langle z \rangle - z]$ to the disorder averaged position $\langle z \rangle$, which in turn is determined self-consistently by the single realisations.

Apart from the correlation length ℓ of the disorder, there is another important length scale in the system. In the absence of any driving force (i.e. $h=0$), we can easily determine the mean deviation of the coordinate z of a special realisation from the disorder averaged position $\langle z \rangle$. For $h=0$ we expect $\dot z=0$, at least in the steady state and (4) straightforwardly leads to

$$\langle (\langle z \rangle - z)^2 \rangle \simeq \frac{\eta^2}{c^2}.$$

So, η/c measures the modulus of the average distance from the common mean. We will see below, that η/c is an upper bound in the case, that the system moves under the influence of a non-zero driving $h \neq 0$.

A word on notation: The disorder averaged velocity $v = \langle \dot z \rangle$ will be denoted by the symbol v.

III. PERTURBATION THEORY

A. Diagrammatic expansion

The differential equation of motion (4) is non-linear, and due to the influence of the solution on the disorder it is impossible to solve it exactly. An ansatz is, to attempt an expansion in the disorder strength η. Therefore, we decompose $z = Z + \zeta$, where $Z = hF(t)$ (with $\partial_t F(t) = f(t)$) is the solution of the non-disordered problem ($\eta = 0$) around which we expand, and

$$\zeta = \sum_{k=1}^{\infty} \zeta_k \eta^k, \quad \langle\zeta\rangle = \sum_{k=1}^{\infty} \langle\zeta\rangle_k \eta^k.$$

is the perturbative correction. Still, we have the equations for ζ_k depending on $\langle\zeta\rangle_k$, which is also unknown. This eventually leads us to a set of two coupled equations

$$(\partial_t + c)\zeta = c\langle\zeta\rangle + \eta \cdot g(Z+\zeta) \tag{8}$$
$$\partial_t \langle\zeta\rangle = \eta \cdot \langle g(Z+\zeta)\rangle, \tag{9}$$

that we can solve iteratively for every order of the perturbation series, if we expand

$$g(Z+\zeta) = \sum_{n=0}^{\infty} \frac{g^{(n)}(Z)}{n!} \zeta^n. \tag{10}$$

If one is interested to keep small orders, this expansion of the disorder can only work if $\zeta \ll \ell$, because ℓ is the typical scale on which $g(z)$ changes. We will come back

to that point, when discussing the special cases for $f(t)$ in sections IV and V. For the moment, we just do it.

The propagator corresponding to the left hand side of Eq. (8) reads

$$G(t) = \Theta(t) \cdot e^{-ct}.$$

Using this propagator, we can formally write down the solution and express it order by order in a power series in η. Up to the second order, the solutions are

$$\langle\zeta\rangle_1(t) = 0, \tag{11}$$

$$\zeta_1(t) = \int_0^t dt_1\, e^{-c(t-t_1)} g(Z(t_1)), \tag{12}$$

$$\langle\zeta\rangle_2(t) = \int_0^t dt_1 \int_0^{t_1} dt_2\, e^{-c(t_1-t_2)} \Delta'[Z(t_1) - Z(t_2)], \tag{13}$$

$$\zeta_2(t) = \int_0^t dt_1 e^{-c(t-t_1)} \left[c\langle\zeta\rangle_2(t_1) + g'(Z(t_1)) \cdot \zeta_1(t_1)\right]. \tag{14}$$

Since we assume Gaußian disorder, the disorder averaged corrections $\langle\zeta\rangle_n$ vanish for odd n. Due to the nested structure, a diagrammatic representation of the perturbation expansion seems most suited. For the interesting quantities $\langle\zeta\rangle_k$, the first two non-vanishing orders are given by:

$$\tag{15}$$

The diagrammatic rules are fairly simple: we draw all rooted trees with k vertices, and add a stem. Each vertex corresponds to a factor $g^{(m)}(Z(t))/m!$, where m counts the number of outgoing lines (away from the root). The line between two vertices represents a propagator $G(t)$. Then Wick's theorem is applied to carry out the disorder average. Each two vertices, that are grouped together for

the average, will be connected by a dashed line. Finally, we replace every straight line which, upon removing it, makes the whole graph falling apart into two subgraphs, by a curly line, corresponding to the propagator of (9), which is just a Heaviside function $\Theta(t)$. In the framework of equilibrium quantum statistical physics, those graphs that involve an internal curly line are called one-particle

reducible (1PR). In our classical problem loops only occur due to the dashed lines originating from the Gaußian average.

B. Consistency of the perturbative series

The perturbation expansion leaves some questions, that have to be addressed. It is not immediately obvious, that taking the disorder average of (14) gives the result in (13), i.e. $\langle \zeta \rangle_2 (t) = \langle \zeta_2(t) \rangle$. However, a short calculation, using integration by parts reveals this relation to hold.

Another, much deeper problem is related to the diagrams involving a curly line in their interior. Due to the curly line, they grow linearly in time. In the following, we call diagrams non-regular, if they correspond to terms which grow unboundedly in time. Koplik and Levine [26] explicitly checked for a time independent driving up to sixth order, that the problematic terms of the diagrams mutually cancel. We give a very general version, that holds for any $f(t)$ and covers all perturbative orders. To illustrate, how this works, we present the calculation for the fourth order here. The somewhat technical induction step, which extends our argument to all orders is given in appendix A. For simplicity, we work with the velocity diagrams, that are obtained by just removing the curly line from the root.

$$2 \cdot \text{[diagram]} = \int_0^t dt_1 \, e^{-c(t-t_1)} \Delta''[Z(t) - Z(t_1)] \int_0^t dt_2 \int_0^{t_2} dt_3 \, e^{-c(t_2-t_3)} \Delta'[Z(t_2) - Z(t_3)]$$

$$\text{[diagram]} = \int_0^t dt_1 \, e^{-c(t-t_1)} (-\Delta''[Z(t) - Z(t_1)]) \int_0^{t_1} dt_2 \int_0^{t_2} dt_3 \, e^{-c(t_2-t_3)} \Delta'[Z(t_2) - Z(t_3)]$$

$$= -2 \cdot \text{[diagram]} + S$$

$$S = \int_0^t dt_1 \int_0^{t_1} dt_2 \, e^{-c(t-t_2)} \Delta''[Z(t) - Z(t_2)] \int_0^{t_1} dt_3 \, e^{-c(t_1-t_3)} \Delta'[Z(t_1) - Z(t_3)]$$

The modification of the second diagram to express it as the sum of the first and S is merely integration by parts. The term S now corresponds to the sum of the two diagrams. It is not straightforward to see, how S behaves generally, but it is easy to see, that it remains bounded for large times. Every time integral carries an exponential damping term. Basically, we have thereby established, that at least up to the fourth order, the perturbation series exists and is well-behaved in the sense, that there are no terms that lead to an overall unbounded growth in time.

Our analysis how the cancellations among non-regular diagrams (i.e. those that involve an internal curly line) generalise to higher orders is presented in appendix A.

IV. TIME-INDEPENDENT DRIVING FORCE

Let us consider the mean field equation (4) for the special choice $f(t) = 1$. Particular cases of this problem have already been addressed [8, 24, 25, 26, 27]. Assuming that the disorder correlator is cusped, e.g.

$$\Delta_{\mathrm{c}}(z - z') = \exp\left[-\frac{|z - z'|}{\ell} \right], \tag{16}$$

it is expected, that the system, described by (4) shows a depinning transistion. The special feature of a cusped disorder potential is, that the resulting disorder force $g(z)$ exhibits jumps. At such jumps, the system is pinned and a finite threshold force is needed to move it in a certain direction. The critical depinning force has been determined in [8] for the parabolic scalloped potential and for a three-state random field model in [27]. In both works, the critical exponent was found to be $\beta = 1$.

For a disorder correlator given by (7), numerical investigations suggest, that pinning is exponentially suppressed for large c. More precisely, the depinning field h_{p} obeys $h_{\mathrm{p}} \propto \exp[-C \cdot c\ell/\eta]$ with some numerical prefactor C. This is reasonable, since η/c is a measure for the typical deviation of each single realisation from the mean, so for $\eta/c \ll \ell$, the system is prevented from adopting to the minima of the disorder potential by the elastic force. Thus, pinning should be diminished. On the other hand, for $\eta/c > \ell$, the equilibrated system for $h = 0$ does place itself at the local disorder minima (for all re-

alisations), since on a scale ℓ it is expected to find a local minimum. So the existence of a finite perceptible threshold force h_{p} is possible for small enough c. Fisher [25] analytically found a threshold field for bounded disorder (strong enough) in the case of charge density waves. The critical exponent has been found to be $\beta = 3/2$ for the smooth disorder potential, in contrast with $\beta = 1$ for the cusped case. Thus, as pointed out in [8], the exponents for the depinning transition in the mean-field case are non-universal.

Well above the depinning threshold, i.e. for $h \gg h_{\mathrm{p}}$, perturbation theory should give a good estimate of the mean velocity. However, it is not clear, why our perturbative approach via a systematic expansion in the disorder (essentially equal to the calculations in [26]) can work, since truncating the Taylor expansion (10) at a finite order is only a good estimate, if $\zeta \ll \ell$. But, the true velocity v is certainly different from h, thence $\zeta = (v-h)t$ grows linearly in time. In appendix B we illustrate, how a resummation of the perturbation scheme leads to a perturbative programme that works. To take only small orders into account a necessary condition is that $\eta/c \ll \ell$. Choosing (7) for the disorder correlator, the first non-vanishing order reads

$$\frac{v}{h} = 1 - \frac{\eta^2}{vh} \left[1 - \phi \left(\frac{c\ell}{2v} \right) \right] + \mathcal{O} \left(\frac{\eta^4}{hv^3} \right), \qquad (17)$$

where we have introduced the function

$$\phi(x) = \sqrt{\pi} \cdot x \, \exp\left(x^2\right) \, [1 - \mathrm{erf}(x)] \qquad (18)$$

for convenience. Its asymptotic expansion reads

$$\phi(x) = \begin{cases} \sqrt{\pi}x - 2x^2 + \mathcal{O}(x^3) & x \ll 1 \\ 1 - \frac{1}{2x^2} + \mathcal{O}(x^{-4}) & x \gg 1 \end{cases}.$$

For $\ell \to \infty$, in (17) all perturbative corrections vanish, hence we get $v = h$. This was expected, since, if the disorder force is correlated over an infinite range, it is essentially constant. Taking the average over all possible values of the disorder (positive and negative) gives zero, hence there is no disorder effect any more. For finite ℓ the velocity is reduced, the smaller $c\ell$, the more. For large $h \gg h_{\mathrm{p}}$, the difference $h - v$ is expected to be small, hence it does not cause much harm if one replaces v by h on the right hand side of (17), rearriving at the explicit expansion in the disorder.

The results from above mainly agree with those in [26]. The major difference is, that Koplik and Levine have been working with $\Delta_{\mathrm{c}}/(2\ell)$ instead of (7) and therefore get an expansion in $\eta^2/(\ell h^2)$, whereas we have a power series in η^2/h^2.
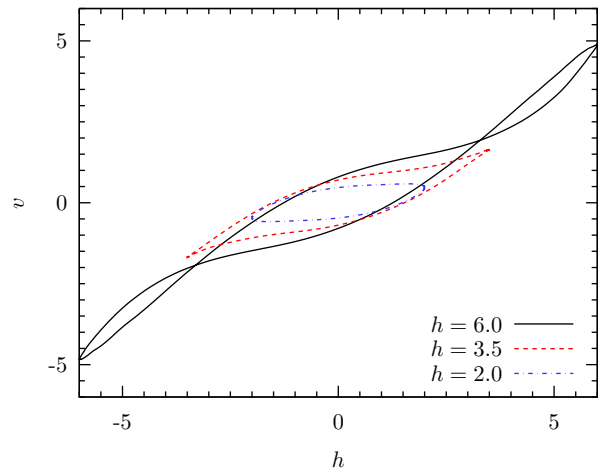

FIG. 1: Numerical solution of (19) for different driving field strengths and $c = 1.0$, $\eta = 2.5$. For the simulation, t and z are measured in units such that $\omega = \ell = 1$.

V. CONSIDERATIONS FOR AC DRIVING FORCES

A. Qualitative behaviour and numerical results

To get an idea about how the system, corresponding to the equation of motion with an ac-driving (cf. (4))

$$\partial_t z = c \cdot [\langle z \rangle - z] + h \cdot \cos \omega t + \eta \cdot g(z) \qquad (19)$$

behaves, we implemented a numerical approach. The disorder is modelled by concatenated straight lines, the values of the junction points are chosen randomly from a bounded interval. The correlator has been checked to be perfectly in agreement with (7).

Before discussing the numerical trajectories, we note a first property of the equation of motion (19). It contains a symmetry of the (disorder averaged) system, namely that all disorder averaged quantities are invariant under the transformation $h \to -h$ and $z \to -z$, which implies $v \to -v$. We have hereby fixed the initial condition to be $z(0) = 0$ for all realisations. If one chooses another initial condition, its sign has to be inverted as well, of course. In the steady state, i.e. for $t \gg c^{-1}$ (as c^{-1} is the time-scale on which transience effects are diminished, see below), the trajectory must therefore obey the symmetry $h \to -h$, $v \to -v$. This symmetry is obviously reflected in the numerical solutions (see fig. 1).

An interesting consequence of this symmetry is, that the even Fourier coefficients of the solution $v(t)$ (which is periodic with period $2\pi/\omega$) vanish. Once the steady state is reached, the symmetry requires $v(t) = -v(t + \pi/\omega)$.
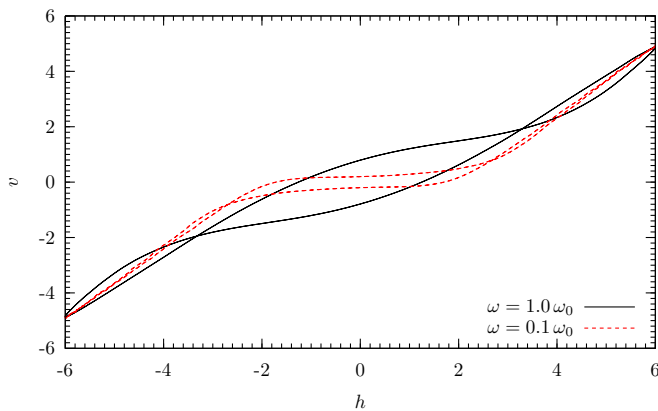
FIG. 2: Numerical solution of equation (19) for $h = 6.0$, $c = 1.0$ and $\eta = 2.5$ for different frequencies, t and z being measured in units such that $\omega_0 = \ell = 1$.

FIG. 3: Numerical solution of equation (19) for different elastic constants and $h = 40.0$, $\eta = 10.0$. The units of t and z are chosen such that $\omega = \ell = 1$.

For the even Fourier modes this means

$$
\begin{aligned}
c_{2N} &= \int_0^{\frac{2\pi}{\omega}} \mathrm{d}t \, v(t) \mathrm{e}^{\mathrm{i}2N\omega t} \\
&= \int_0^{\frac{\pi}{\omega}} \mathrm{d}t \, v(t) \mathrm{e}^{\mathrm{i}2N\omega t} + \int_0^{\frac{\pi}{\omega}} \mathrm{d}t \, v\left(t + \frac{\pi}{\omega}\right) \mathrm{e}^{\mathrm{i}2N\omega t} = 0.
\end{aligned}
$$

The typical picture of a v-h-plot is that of a single hysteresis for $h \ll \eta$ and a double hysteresis for $h \gg \eta$. In an intermediate range, we find a single hysteresis with a cusped endpoint. The qualitative shape of the solution trajectories agrees with numerical results [31, 32], that have been obtained as solutions for (1) in the case of finite interfaces with periodic boundary conditions. Moreover, as the frequency is sent to zero $\omega \to 0$, the hysteretic trajectory approaches the depinning curve for an adiabatic change of the driving field. This is shown in fig. 2.

In the following, we want to give a qualitative discussion of the hystereses in the case of small elasticity c.

Weak fields $h \ll \eta$: In the case of weak driving fields, the typical system in a certain disorder configuration remains in a potential well of the disorder. The elastic force may slightly shift the centre around which $z(t)$ oscillates, but this is not very important, since we can instead think of an effective potential. To understand the hysteretic behaviour, it is instructive to think of the force field $g(z)$ instead of the potential. Starting at $h(t) = 0$ for large enough t (i.e. in the steady state) we expect a certain realisation to be located at the zero point $g(z_0) = 0$ of a falling edge, since this corresponds to a stable configuration. As the field grows, the system starts to move in the direction of growing z, where the disorder force competes with the driving. Because in the vicinity of the potential minimum, the disorder force $g(z)$ behaves approximately linear in z, the acceleration is approximately zero and the velocity almost constant. This changes when the driving is about to reaching its maximum. The slower
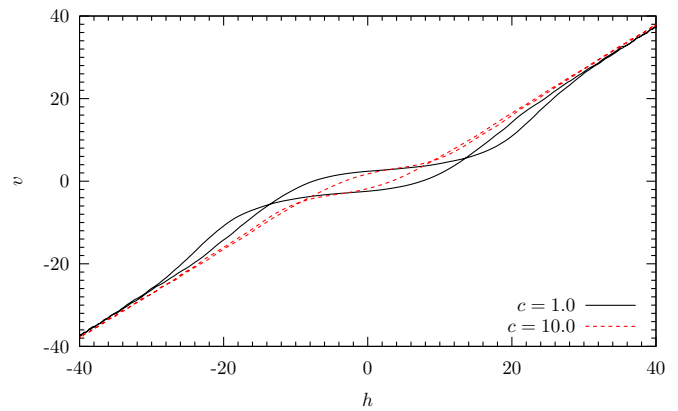
the growth, the smaller the velocity. At the maximum, the velocity equals zero, as the driving and the restitutional disorder force compensate. For decreasing $h(t)$, the restitution force wins and pushes the system back in the direction of the potential minimum. Hence, the velocity v turns negative short-time after the field has reached its maximum and is still positive. Once the stable position z_0 is reached again, the same starts in the negative direction.

Certainly, the restitutional disorder force need not continuously grow with z, but may exhibit bumps or similar noisy structure, but those details average out when taking the mean over all disorder configurations.

Strong fields $h \gg \eta$: In the case of strong driving amplitudes, we encounter the situation of a double hysteresis. Again, starting at $h(t) = 0$ for $t \gg c^{-1}$, we assume the system to be located at the zero $g(z_0) = 0$ of a falling edge of the (effective) disorder force field. As $h(t)$ grows, we first have the same situation as in the case of weak driving: The disorder acts restitutionally and thus keeps the velocity small and leads to a small slope $\mathrm{d}v/\mathrm{d}h$. Once the field is of the order η, the typical maximum of a disorder force, the system is no longer locked into a potential well, but a cross-over to sliding behaviour sets in. On further increasing h, the system finally arrives at a slope $s = \mathrm{d}v/\mathrm{d}h$, which depends mainly on η and c. After the field reaches its maximum, the velocity decreases with the field, the slope being $\mathrm{d}v/\mathrm{d}h \approx s$, also if this slope has been different just before the field amplitude has been reached. This slope approximately remains, until the field is weaker than the typical disorder force, when the system is again trapped in a potential well. Since on rising edges of the disorder force, driving and disorder point in the same direction, the system will rarely sit there (it moves away very fast). The velocity becomes negative before $h = 0$, since the system slides down the falling edge ($\mathrm{d}g/\mathrm{d}z < 0$) of the disorder force. At $h = 0$ everything starts again in the negative direction. An example for fairly large field amplitudes is shown in fig. 3.

So far, our discussion has emphasised on small c by absorbing its effect into an effective disorder picture. The effect of larger c is to couple the configuration $z(t)$ of every realisation strongly to the mean $\langle z(t) \rangle$. This wipes out the effect of disorder in the time regime when $h(t)$ takes on small values. As we have discussed above, in those time intervals the possibility to explore the shape of the individual disorder landscape plays an important rôle. Thus for larger c the double hysteresis winds around a straight line, connecting the extremal velocities. This can be seen in fig. 3.

B. Validity of perturbation theory

For an oscillating driving force, the question is still open, whether one may assume ζ to be small compared to ℓ. If c is large, any particle moving in a particular realisation of a disorder potential is strongly bound to the disorder averaged position. This prevents it from exploring the own disorder environment and thus large c effectively scale down η. All realisations stay close to the disorder averaged position, the mean deviation being η/c. A problem now occurs, if the disorder averaged position deviates strongly from the $\eta = 0$ solution. For $h \gg \eta$ this can only happen during those periods, where $h \cos \omega t$ takes on small values. The time, that has to elapse, until every system has adopted to its own disorder realisation, and hence the time until the system can be pinned, is c^{-1} (see below). For perturbation theory to work, this time must be large compared to the length of the period during which $h \leq \eta$, which we roughly estimate as $\eta/(\omega h)$. This gives us a second condition for the applicability of perturbation theory: $h/\eta \gg c/\omega$.

In summary, the conditions for perturbation theory to hold are the following. The driving force amplitude h has to be large compared to η, $h/\eta \gg \max\{c/\omega, 1\}$ to make the series expansion work and to guarantee that the disorder averaged solution stays close to the $\eta = 0$ trajectory (around which we expand). Moreover, c must be large ($c \gg \eta/\ell$) to ensure proximity of each realisation to the disorder average.

C. Simple perturbative estimates

Before embarking on conclusions that can be drawn from the perturbative solution of the equation of motion (4), we shall determine the typical deviation of the position of a single realisation $z(t)$ from the mean $\langle z(t) \rangle$.
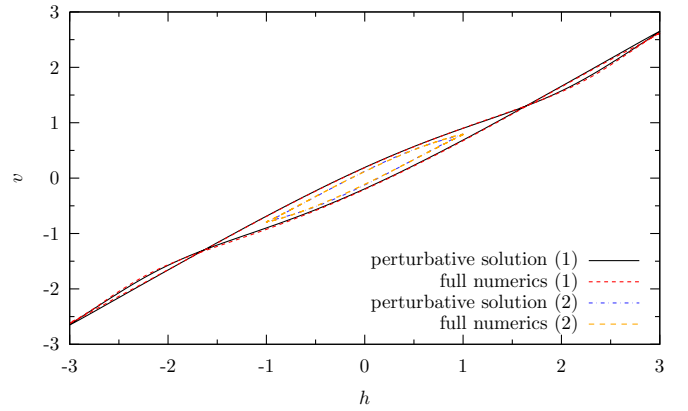

FIG. 4: Comparison of the numerical solution of equation (19) with the result obtained from the first non-vanishing perturbative order for (1) $h = 3.0$, $c = 3.0$, $\eta = 1.5$ and (2) $h = 1.0$, $c = 1.0$, $\eta = 0.6$. The units of t and z are chosen such that $\omega = \ell = 1$.

This has the following bound

$$
\begin{aligned}
\langle (\langle z \rangle - z)^2 \rangle &= \eta^2 \langle \zeta_1^2 \rangle + \mathcal{O}(\eta^4) \\
&= \eta^2 \int_0^t dt_1 dt_2 \, e^{-c(2t - t_1 - t_2)} \Delta[Z(t_1) - Z(t_2)] \\
&\leq \int_0^t dt_1 dt_2 \, e^{-c(2t - t_1 - t_2)} = \frac{\eta^2}{c^2} \left(1 - e^{-ct}\right)^2 .
\end{aligned}
\tag{20}
$$

The estimate simply replaces the disorder correlator Δ by its maximum and therefore gives an upper bound. Strictly, it is only true to order $\mathcal{O}(\eta^2)$. This confirms our claim from section II, that an estimate for the mean deviation from the averaged solution is given by η/c.

D. Perturbative harmonic expansion

As has been discussed in section V B, for $h/\eta \gg \max\{c/\omega, 1\}$ and $\eta/(c\ell) \ll 1$, perturbation theory should do pretty well. A direct comparison, shown in fig. 4, confirms an excellent agreement. So, at least for weak disorder, when perturbation theory is valid, one can hope to extract some information from the lowest order. For an ac driving force, even this lowest perturbative order for the velocity is a very complicated expression. The diagrammatic prescription yields up to the order $\mathcal{O}(\eta^2)$

$$
v(t) = h \cos \omega t + \eta^2 \int_0^t dt' \, e^{-c(t-t')} \Delta'[Z(t) - Z(t')]. \tag{21}
$$

Remember, that $Z(t) = (h/\omega) \sin \omega t$ is the solution for the problem without disorder, around which we expand. It seems reasonable to aim a harmonic expansion of the

mean velocity v. The ansatz therefore is

$$v(t) = \sum_{N=1}^{\infty} \left[a_N \cos N\omega t + b_N \sin N\omega t\right], \qquad (22)$$

for N odd. Recall, that, for reasons of the $h \to -h$ and $v \to -v$ symmetry of the trajectory, which has been discussed in the previous section, the Fourier coefficients for even N vanish.

Starting from the first order result for v (21), we express the disorder correlator by its Fourier transform

$$\Delta'[Z(t) - Z(t')] = \int \frac{dq}{2\pi}(iq)\Delta(q)e^{iq\frac{h}{\omega}[\sin \omega t - \sin \omega t']} \quad (23)$$

and expand the exponential term in a double Fourier se-

ries in t and t', respectively:

$$e^{ia \sin \omega t} = \sum_{n=-\infty}^{\infty} J_n(a)e^{in\omega t}$$

$$\int_0^t dt' \, e^{-c(t-t')-ia \sin \omega t'} = \sum_{n=-\infty}^{\infty} J_n(-a)\frac{e^{in\omega t} - e^{-ct}}{c + in\omega}.$$

Here, $J_n(a)$ are the Bessel functions of the first kind. As we are interested only in the behaviour for large enough times (the steady state solution), we remove all terms that are damped out exponentially for $t \gg c^{-1}$ from the very beginning. Note, that c^{-1} is indeed the time scale for the transience, as has been claimed before.

For the mean velocity, we obtain

$$v(t) = h \cos \omega t + \eta^2 \sum_{m,n=-\infty}^{\infty} \int \frac{dq}{2\pi}(iq)\Delta(q)J_m\left(q\frac{h}{\omega}\right)J_n\left(-q\frac{h}{\omega}\right)\frac{e^{i(m+n)\omega t}(c - in\omega)}{c^2 + n^2\omega^2} \qquad (24)$$

In principle, this is already a Fourier series representation, not very elegant, though. The argument $(m+n)\omega t$ of the expansion basis exponentials promises a rather complicated structure for the coefficients. A first observation, however, can already be made: Under the q integral we find an odd function $(iq)\Delta(q)$ and a product of two Bessel functions of order m and n, respectively. For the q-integral to result in a finite value, a function is required

that is not odd in q. This necessitates the product of the two Bessel functions to be odd, or, equivalently, $m + n$ to be an odd number. Whence, we conclude, that to first perturbative order, our symmetry argument (Fourier coefficients for even N must vanish) is fulfilled exactly.

It requires some tedious algebra to collect all contributions belonging to a certain harmonic order from the double series. Eventually, we obtain the series expansion

$$\frac{v(t)}{h} = \cos \omega t + \sum_{N=1}^{\infty} \left[A_N \cos N\omega t + B_N \sin N\omega t\right] \qquad (25)$$

$$A_N = 2\frac{\eta^2}{h^2}\frac{\omega^2}{c^2}\left[\sum_{n=1}^{N-1}\frac{(-1)^n n K_{N-n,n}}{1 + n^2\omega^2/c^2} - \sum_{n=1}^{\infty}\frac{n K_{N+n,n}}{1 + n^2\omega^2/c^2} - \sum_{n=N}^{\infty}\frac{n K_{n-N,n}}{1 + n^2\omega^2/c^2}\right] + \mathcal{O}(\eta^4) \qquad (26)$$

$$B_N = 2\frac{\eta^2}{h^2}\frac{\omega}{c}\left[-\sum_{n=1}^{N-1}\frac{(-1)^n K_{N-n,n}}{1 + n^2\omega^2/c^2} - \sum_{n=0}^{\infty}\frac{K_{N+n,n}}{1 + n^2\omega^2/c^2} + \sum_{n=N}^{\infty}\frac{K_{n-N,n}}{1 + n^2\omega^2/c^2}\right] + \mathcal{O}(\eta^4) \qquad (27)$$

For convenience, we introduced the following abbreviation (depending only on the parameter ratio $h/(\omega\ell)$), in which $_3F_3$ denotes the generalised hypergeometric function [33].

$$K_{m,n} = \frac{h}{\ell}\int\frac{dq}{2\pi}\,q\Delta(q)\cdot J_m\left(q\frac{h}{\omega}\right)J_n\left(q\frac{h}{\omega}\right) \qquad (28)$$

$$= 2\left(\frac{h}{\omega\ell}\right)^{m+n+1}\frac{\Gamma([m+n+2]/2)}{\sqrt{\pi}\cdot m!\cdot n!}\times \qquad (29)$$

$$_3F_3\left[\left\{\frac{m+n+1}{2},\frac{m+n+2}{2},\frac{m+n+2}{2}\right\},\{m+1,n+1,m+n+1\},-\frac{4h^2}{\omega^2\ell^2}\right].$$

Note, that taking $\omega \to 0$ is forbidden here, as we used $\omega \neq 0$ while deriving the coefficients and moreover per-
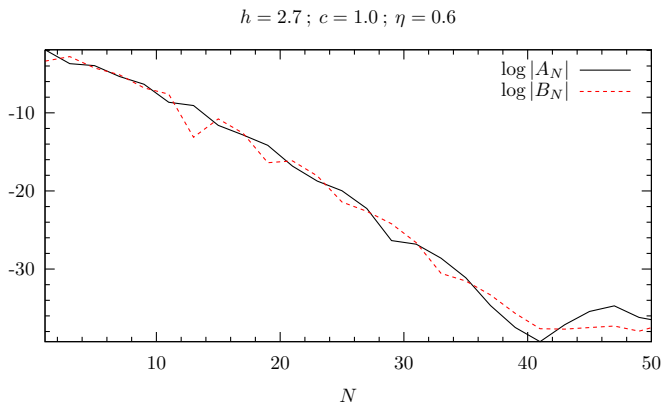
FIG. 5: Plotting the logarithms of $|A_N|$ and $|B_N|$ reveals the exponential decay with N. In the regime where numerical errors do not dominate the result, a linear regression seems appropriate.
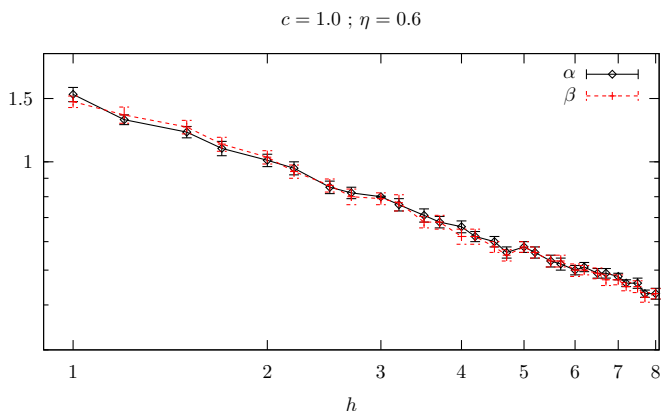

FIG. 6: Performing the linear regression for many h yields slopes α and β appearing to depend on h in a power-law fashion.

turbation theory breaks down (recall that $h/\eta \gg c/\omega$). The same holds for $\ell \to 0$. The remaining extreme limits $\omega \to \infty$ and $\ell \to \infty$ are not interesting, since in these limits the disorder is rendered unimportant. Therefore, in the following, we assume finite (positive) values for ℓ and ω and moreover set them equal to one $\omega = \ell = 1$, by appropriately choosing the units for z and t.

Now, we are left with three dimensionless parameters: h, c and η. The dependence of the first order perturbative Fourier coefficients on η is trivial. The dependence on c is also evident, as can be read off from (26,27). For larger c, the system is more tightly bound to the non-disordered solution, supressing perturbative corrections.

The most interesting but also the most difficult is the dependence of the Fourier coefficients on h. Actually, there are two competing effects. On the one hand, large driving strengths render the disorder unimportant in all cases accessible through perturbative methods. In a nutshell, the expansion parameter is η/h. On the other hand, if one thinks of $g(Z(t))$ as a function of time, the more rapid $Z(t)$ changes the more g fluctuates on short

time scales and thus brings higher frequency contributions to $v(t)$. The first remark is reflected in the overall weight of the Fourier coefficients as corrections to the non-disordered case, decreasing with h. The second idea is expected to express itself in the decay of the Fourier coefficients with N. The larger h, the weaker we expect this decay to be.

In equations (25) and (28), the dependence of the higher harmonics on h is hidden in the $K_{m,n}$ as functions of h: The maximum of the $K_{m,n}$ as functions of the parameter $h/(\omega \ell)$ shifts to larger values as m or n increase. In the integral representation this can be seen, as the Bessel functions take their first extrema at large arguments for large indices. However, the complicated way in which the $K_{m,n}$ functions enter A_N and B_N hinders an analytic access to the decay law. A numerical determination of the Fourier coefficients for the perturbative result reveals an exponential decay, cf. fig. 5. The noisy behaviour for $N \geq 40$ is due to numerical fluctuations. Note, that these fluctuations are of the order 10^{-14}, which is quite reasonable. The plot in fig. 5 is mere illustration of a more general phenomenon. This exponential decay has been found for many sets of parameters, thus one is led to the ansatz

$$|A_N| \sim \mathrm{e}^{-\alpha N} \quad ; \quad |B_N| \sim \mathrm{e}^{-\beta N}, \qquad (30)$$

where α and β can be estimated through a linear regression up to a suitable $N_{\max}$. Of course, it is not expected, that α and β are distinct, nor that they depend on the parameters in different ways. Determining both just doubles the amount of available data.

As our results are first-order perturbative, α and β must not depend on η. The main interest now focusses on the dependence of the decay constants on h. The results from a linear regression for a series of h-values, c and η kept fixed, suggest a power-law dependence

$$\alpha(h) = C_\alpha \cdot h^{-\xi_\alpha}, \quad \beta(h) = C_\beta \cdot h^{-\xi_\beta}. \qquad (31)$$

Fig. 6 displays this relation for a particular example. Repeating this data collection and subsequent regression for different values for c and η yields the results summarised in table I. While the exponent ξ appears constant $\xi \approx 0.6$, the prefactor seems to depend on c. An attempt to redo the same procedure, done for h, with the parameter c to gain information about the functional dependence of α and β on c yields a complicated but rather weak dependence, which gives no further insight. The obvious approach is to visualise the dependence of C_α and C_β on c. The linear fit in fig. 7 gives a fairly tiny slope, so the dependence of the decay constants on c may be assumed to be weak.

Certainly, it is desirable to ascertain the validity of this decay law beyond perturbation theory. In a few words, it ought to be explained, why we have not been able to do it. First of all, the logarithmic plots of the Fourier coefficients in fig. 5 exhibit fluctuations around the linear decrease. This "noise" is authentic and not attributed

TABLE I: Results for the regression (31).

c	η	C_α	C_β	ξ_α	ξ_β
1.0	0.6	1.52	1.52	0.61	0.61
1.5	0.6	1.56	1.56	0.58	0.59
2.0	0.6	1.56	1.59	0.58	0.60
2.5	0.6	1.63	1.62	0.61	0.61
3.0	1.0	1.66	1.66	0.63	0.63
3.5	1.0	1.71	1.68	0.62	0.62
4.0	1.0	1.69	1.65	0.61	0.60
4.5	1.0	1.72	1.68	0.62	0.62
5.0	2.0	1.71	1.67	0.61	0.60
5.5	2.0	1.73	1.73	0.61	0.62
6.0	2.0	1.77	1.72	0.62	0.62
6.5	3.0	1.76	1.77	0.62	0.62
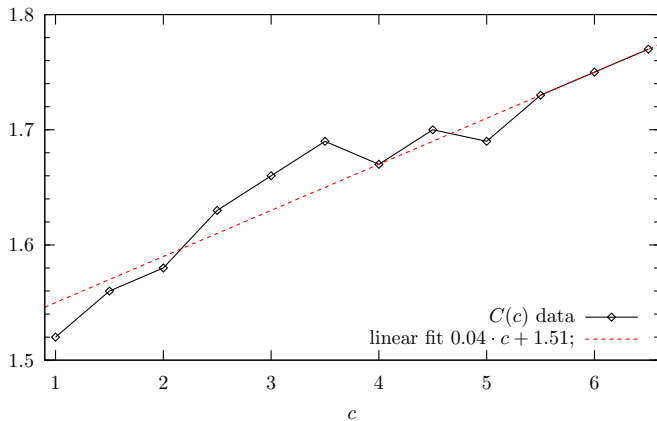
FIG. 7: Plot of the change of the prefactor $C(c)$ in (31) on c. The linear fit yields a fairly tiny slope.

to numerical inaccuracies. The exponential decay of the Fourier coefficients is superimposed on a true, complicated dependence. Hence, it requires a lot of data points to obtain reasonable data. Since the Fourier coefficients for even N vanish, in the example of fig. 5 the regression can be carried out over around 15-20 data points. This is a fair number. The quality relies heavily on the accuracy of the numerical determination of the Fourier coefficients. In Fourier analyses of the numerics for the full equation of motion (19), we did not manage to get a precision better than of the order of 10^{-3}. This means, the regression has to be stopped at $N_{\max}$, where $\log A_{N_{\max}} \approx -7$. In the example of fig. 5, this leaves us with less than 5 data points. In view of the natural fluctuations, a linear regression is not sensible any more.

VI. CONCLUSIONS

The mean-field version of the problem of ac-driven elastic interfaces in disordered media admits a regular perturbative treatment that, where applicable, agrees very well with the numerics for the full equation of motion. It has been shown, that diagrammatic contributions with

an unbounded increase in time cancel among each other, leaving a well-behaved perturbative expansion.

The solutions to the mean-field equation of motion are found to share many features with the numerical solutions of the original problem, like the hysteretic behaviour of the v-h-plots.

Unfortunately, the perturbative expressions are very complicated and thus only of little use for analytic insights. However, they improve numerical results tremendously which made possible to establish the dependence of the decay constants of the Fourier modes on h as a power law $\alpha, \beta(h) = C(c) \cdot h^{-\xi}$ with $\xi \simeq 0.6$.

APPENDIX A: REGULARITY OF THE PERTURBATION EXPANSION

In section III B we have analysed, how the unbounded contributions, contained in the two diagrams that involve a curly line, mutually cancel in the second non-vanishing perturbative order. In this appendix, we are going to explain how this cancellation process generalises to all orders in perturbation theory. As before, for simplicity, we work with the diagrams for the disorder-averaged velocity, that arise by just removing the curly lines from the root of the diagrams for $\langle \zeta \rangle$ (cf. equation (15)). In a velocity diagram contributing to the n-th order (recall, that only for even n the corrections are non-zero), any curly line connects two trees of order p and q (both even) with the restriction $p + q = n$. Both trees appear in the expansion of lower orders, namely p and q, respectively. In the following, we want to sketch an inductive proof for the claim that the unbounded terms originating from trees with curly internal lines cancel among each other.

Let us assume, that for order n we have achieved to ensure regularity. For every unbounded tree T, there is thus a set $T^1, \ldots, T^a$ of, let us call them *cancelling trees*, such that $T + T^1 + \ldots + T^a$ is a regular, bounded expression in time. As a starting point for the induction, take $n = 4$, where the validity of the claim has been verified in section III B. It is now the task to validate the regularity for order $n + 2$. First of all, we consider the process of attaching the root of a regular tree S (with no internal curly line) of order s by a curly line to a vertex v of another regular tree R of order $r = n + 2 - s$ to obtain a new irregular tree A of order $n + 2$. The vertex v must be connected to another vertex $w \in R$ by a dashed line, to carry out the Gaußian disorder average. Without loss of generality, we assume that v is connected to w by a

path that first makes a step towards the root. The rules for the diagrammatic expansion ensure, that there is a maximal regular subtree $T \subset R$, which contains v and w.

Using partial integration, it is possible to move the vertex to which S is connected (via the curly line) to a neighbouring vertex in T. Thus, it is possible to move the connection vertex along the unique way (in T) from v to w. We are going to show, that once w is reached, we have obtained the cancelling tree which is unique. Diagrammatcially, the process of moving the connection vertex from v to w reads:
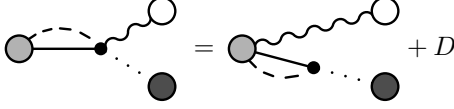
Here, the blank circle represents S, the lightgrey circle

stands for the subtree R_1 of R, to which v connects and the darkgrey shaded circle denotes trees which run out of v (summarised in the following as R_2). Certainly, in general there may be dashed lines between the dark- and the lightgrey circle, which we have omitted as they are not relevant for the forthcoming discussion. The dotted line just serves as a joker - it is not important to specify how many trees go out of v. The last term D collects the left-over terms from the partial integration. Note, that, if it takes several steps to go from v to w, the intermediate expressions (in the partial integration) are no valid diagrams.

To illustrate the procedure, we take a look at the first step:

$$= R_1(t) \int_0^{T_1} dt_1\, e^{-c(T_1-t_1)}(-1)^\nu \Delta^{(\mu+\nu)}[Z(\tau)-Z(t_1)]R_2(t_1) \int_0^{t_1} dt_2 S(t_2)$$

$$= R_1(t) \int_0^{T_1} dt_2 S(t_2) \int_0^{T_1} dt_1 e^{-c(T_1-t_1)}(-1)^\nu \Delta^{(\mu+\nu)}[Z(\tau)-Z(t_1)]R_2(t_1)$$

$$- R_1(t) \int_0^{T_1} dt_1\, e^{-c(T_1-t_1)} S(t_1) \int_0^{t_1} dt_2\, e^{-c(t_1-t_2)}(-1)^\nu \Delta^{(\mu+\nu)}[Z(\tau)-Z(t_2)]R_2(t_2)$$

The order of the derivative (i.e. the number of outgoing lines) of w and v are denoted by μ and ν, respectively. The time, at which the whole diagram is to be evaluated, is t, the time corresponding to the vertex to which v is connected is given by T_1, t_1 is thus the time associated to v and so on. The time of w is τ. Thus, we see, that if w is not the vertex to which v is directly connected (then $T_1 \neq \tau$ in general), the first expression after partial integration cannot be a valid diagram: v has lost one order of derivative ($\nu - 1$ lines go out instead of ν), but the derivative of the correlator Δ has not changed. A valid diagram is then obtained, when the connection of S has reached w. Then, v has lost an outgoing line, but w received one more and we indeed have achieved a cancelling tree: the factor $(-1)^\nu$ remains, the true diagram, however, has $(-1)^{\nu-1}$. The signs are different, thus the two trees cancel. The left-over term from the partial integration is again regular, as can be seen since all time integrals carry an exponential damping term. It is clear, that this is generally true for every partial integration step.

To go one step further, we assume now S to be irregular. Essentially, the same procedure works, but there are more cancelling trees: one has take all cancelling trees $\{S^i\}$ for S into account (which exist by induction hy-

pothesis), thus S is replaced by $\sum S^i$ and thence the left-over terms are again regular.

A possible irregularity of R can be accounted for in the same way. It is, however, important to explain why this is possible, i.e. what is v and w in the cancelling trees for R. In the case of irregular S the problem was easy, since all trees have a unique root. As we have seen already, the procedure of creating cancelling trees does not change the structure of regular subtrees. Thence, all cancelling trees for R contain T. This makes clear, which v and w have to be chosen in the cancelling trees: they are well-defined in T and T is a well-defined subtree of the cancelling trees. Thus, repeating the whole procedure described above for all cancelling trees of R yields the complete set of cancelling trees for A in the most general setting.

APPENDIX B: RESUMMATION OF THE PERTURBATION EXPANSION

For a constant driving force, it is not clear, why a perturbative approach using (10) should work. So, we approach the perturbation expansion from another direction, which will turn out to be a resummation of our

former expansion in the disorder. Take our original equation of motion

$$\partial_t z = c \cdot [\langle z \rangle - z] + h \cdot f(t) + \eta \cdot g(z) \qquad (B1)$$

and decompose $z = X + \xi$, where $X = \langle z \rangle$. Thus $\langle \xi \rangle = 0$. This gives us two non-linearly coupled non-linear differential equations

$$\partial_t X(t) = h \cdot f(t) + \eta \cdot \langle g(X + \xi) \rangle \qquad (B2)$$

$$(\partial_t + c)\xi(t) = \eta \big[g(X + \xi) - \langle g(X + \xi) \rangle \big] \qquad (B3)$$

If c is large enough, one can always achieve $\xi \ll \ell$ and thus a Taylor expansion of the disorder around $X(t)$ keep-

ing only lowest order-terms seems reasonable. Instead of a systematic expansion in the disorder, we now perform power-counting in ξ. This leads to a recursive structure for ξ:

$$(\partial_t + c)\xi = \eta \sum_{n=0}^{\infty} \frac{1}{n!} \left[g^{(n)}(X)\xi^n - \left\langle g^{(n)}(X)\xi^n \right\rangle \right]$$

$$= \eta \left[g(X) + g'(X)\xi - \langle g'(X)\xi \rangle + \frac{1}{2} g''(X)\xi^2 + \dots \right]$$

and thus a self-consistent equation for $X(t)$

$$\partial_t X = h \cdot f(t) + \eta \sum_{n=0}^{\infty} \frac{1}{n!} \left\langle g^{(n)}(X)\xi^n \right\rangle$$

$$= h \cdot f(t) + \eta \left\langle g(X) + \eta g'(X) \int_0^t dt' e^{-c(t-t')} \big[g(X) + \dots \big] + \dots \right\rangle$$

The graphical structure is now similar to that of section III A. It reads

$$\qquad (B4)$$

This series only consists of "irreducible" (1PI) graphs, where no line can be cut such that the whole graph falls apart into two and no curly lines occur. Otherwise the diagrammatic rules are essentially the same as before. Every vertex corresponds to $g^{(m)}(X)/m!$, where m counts the number of outgoing lines. The full lines are propagators of the differential equation (B3) for ξ.

On analysing the expansion of the first and simplest diagram in the disorder (up to $\mathcal{O}(\eta^6)$)

$$g(X) = g(Z + \langle \zeta \rangle) = g(Z) + g'(Z) \langle \zeta \rangle + \dots,$$

one inspects that the "new" diagrammatic expansion (B4) is merely a resummation of our old one. However, if a constant driving force is exerted, $\xi(t)$ remains bounded (and, depending on c, also small) at all times, in contrast to $\zeta(t)$. This can be seen by confirming the earlier

estimate for the mean deviation of a realisation from the mean position (cf. section II), which is exactly ξ. We observe that

$$\langle (\langle z \rangle - z)^2 \rangle = \langle \xi^2 \rangle = \frac{\eta^2}{c^2} \cdot \phi \left(\frac{c\ell}{2v} \right) + \mathcal{O}(\eta^4). \qquad (B5)$$

As $\phi \le 1$, to this order η/c is an upper bound for the typical distance from the mean. Thus this perturbation expansion should work fine for $\eta/c \ll \ell$. As far as there is overlap, this also agrees with the result in [26]. For a constant driving force h, the first order correction to the velocity yields a self-consistent integral equation

$$v = h + \eta^2 \int_0^t dt' \, e^{-c(t-t')} \Delta'[v(t-t')] + \mathcal{O}(\eta^4), \qquad (B6)$$

which has been used in computing equation (17).

[1] S. Brazovskii and T. Nattermann, Adv. Phys. **53**, 177 (2004).

[2] A. A. Middleton, Phys. Rev. B. **45**, 9465 (1992).

[3] S. Lemerle et al., Phys. Rev. Lett. **80**, 849 (1998).

[4] P. Chauve, T. Giamarchi, and P. Le Doussal, Phys. Rev. B **62**, 6241 (2000).

[5] P. Metaxas et al., Phys. Rev. Lett. **99**, 217208 (2007).

[6] S. Bustingorry, A. Kolton, and T. Giamarchi, Eur. Phys. Lett. **81**, 26005 (2008).

[7] T. Nattermann, S. Stepanow, L.-H. Tang, and H. Leschhorn, J. Phys II France **2**, 1483 (1992).

[8] O. Narayan and D. S. Fisher, Phys. Rev. B **46**, 11520 (1992).

[9] D. Ertas and M. Kardar, Phys. Rev. E **49**, R2532 (1994).

[10] H. Leschhorn, T. Nattermann, S. Stepanow, and L.-H. Tang, Ann. Physik (Leipzig) **6**, 1 (1997).

[11] P. Chauve, P. Le Doussal, and K. J. Wiese, Phys. Rev. Lett. **86**, 1785 (2001).

[12] P. Le Doussal, K. J. Wiese, and P. Chauve, Phys. Rev. B **66**, 174201 (2002).

[13] P. Le Doussal, K. J. Wiese, and P. Chauve, Phys. Rev. E **69**, 026112 (2004).

[14] W. Kleemann et al., Phys. Rev. Lett. **99**, 097203 (2007), and references therein.

[15] W. Kleemann, Annu. Rev. Mater. Res. **37**, 415 (2007).

[16] W. Jeżewski, W. Kuczyński, and J. Hoffmann, Phys. Rev. B **77**, 094101 (2008).

[17] F. Schütze, arXiv:0906.1917v1 [cond-mat.dis-nn] (2009).

[18] M. Kardar, Phys. Rep. **301**, 85 (1998).

[19] D. S. Fisher, Phys. Rep. **301**, 113 (1998).

[20] G. Grüner, Rev. Mod. Phys. **60**, 1129 (1988).

[21] G. Blatter et al., Rev. Mod. Phys. **66**, 1125 (1994).

[22] T. Giamarchi and P. Le Doussal, Phys. Rev. Lett **72**, 1530 (1994).

[23] T. Nattermann and S. Scheidl, Adv. Phys. **49**, 607 (2000).

[24] D. S. Fisher, Phys. Rev. Lett. **50**, 1486 (1983).

[25] D. S. Fisher, Phys. Rev. B **31**, 1396 (1985).

[26] J. Koplik and H. Levine, Phys. Rev. B **32**, 280 (1985).

[27] H. Leschhorn, J. Phys. A **25**, L555 (1992).

[28] I. F. Lyuksyutov, J. Phys. C **7**, 7153 (1995).

[29] M. Feigel'man, Sov. Phys. JETP **58**, 1076 (1983).

[30] R. Bruinsma and G. Aeppli, Phys. Rev. Lett. **52**, 1547 (1984).

[31] A. Glatz, T. Nattermann, and V. Pokrovsky, Phys. Rev. Lett. **90**, 047201 (2003).

[32] A. Glatz, Ph.D. thesis, Universität zu Köln (2004).

[33] I. Gradshteyn and I. Ryzhik, *Table of Integrals, Series, and Products* (Academic Press, San Diego, London, 2000), sixth ed.